energies

MDPI

Article

Economic Viability Study of an On-Road Wireless Charging System with a Generic Driving Range Estimation Method †

Aditya Shekhar [1,*,‡], Venugopal Prasanth [1,‡], Pavol Bauer [1] and Mark Bolech [2]

1 Electrical Sustainable Energy, Delft Institute of Technology, Mekelweg 4, Delft 2628 CD, The Netherlands; v.prasanth@tudelft.nl (V.P.); p.bauer@tudelft.nl (P.B.)

2 The Netherlands Organisation for Applied Scientific Research (TNO), Van Mourik Broekmanweg 6, Delft 2628 XE, The Netherlands; mark.bolech@tno.nl

* Correspondence: a.shekhar@tudelft.nl; Tel.: +31-015-2785744; Fax: +31-015-2781182

† This paper is an extended version of our paper published in Shekhar, A.; Prasanth, V.; Bauer, P.; Bolech, M. Generic methodology for driving range estimation of electric vehicle with on-road charging. In Proceedings of the 2015 IEEE Transportation Electrification Conference and Expo (ITEC) and Shekhar, A.; Bolech, M.; Prasanth, V.; Bauer, P. Economic considerations for on-road wireless charging systems—A case study. In Proceedings of the 2015 IEEE PELS Workshop on Emerging Technologies: Wireless Power (WoW).

‡ These authors contributed equally to this work.

Academic Editor: K. T. Chau
Received: 4 September 2015; Accepted: 18 January 2016; Published: 26 January 2016

Abstract: The economic viability of on-road wireless charging of electric vehicles (EVs) strongly depends on the choice of the inductive power transfer (IPT) system configuration (static or dynamic charging), charging power level and the percentage of road coverage of dynamic charging. In this paper, a case study is carried out to determine the expected investment costs involved in installing the on-road charging infrastructure for an electric bus fleet. Firstly, a generic methodology is described to determine the driving range of any EV (including electric buses) with any gross mass and frontal area. A dynamic power consumption model is developed for the EV, taking into account the rolling friction, acceleration, deceleration, aerodynamic drag, regenerative braking and Li-ion battery behavior. Based on the simulation results, the linear dependence of the battery state of charge (SoC) on the distance traveled is proven. Further, the impact of different IPT system parameters on driving range is incorporated. Economic implications of a combination of different IPT system parameters are explored for achieving the required driving range of 400 km, and the cost optimized solution is presented for the case study of an electric bus fleet. It is shown that the choice of charging power level and road coverage are interrelated in the economic context. The economic viability of reducing the capacity of the on-board battery as a trade-off between higher transport efficiency and larger on-road charging infrastructure is presented. Finally, important considerations, like the number of average running buses, scheduled stoppage time and on-board battery size, that make on-road charging an attractive option are explored. The cost break-up of various system components of the on-road charging scheme is estimated, and the final project cost and parameters are summarized. The specific cost of the wireless on-road charging system is found to be more expensive than the conventional trolley system at this point in time. With decreasing battery costs and a higher number of running buses, a more economically-viable system can be realized.

Keywords: analysis; contactless; charging; cost; driving range, dynamic; economic; electric vehicle (EV); extension; emissions; inductive power transfer (IPT); static; viability; wireless

1. Introduction

Transition from over-utilized fossil fuels to cleaner, environment-friendly and more efficient electrical energy has propelled the proliferation of electric vehicles (EVs) in the market. Plug-in vehicles that use electric motors as prime movers have seen rapid mass production since 2011 [1,2]. The implications of the evolution and integration of electric vehicular technology and its associated charging aspects with smart grids and distribution networks has garnered growing interest [3].

Bulk energy consumers, like the transportation sector, if electrified, can yield a more sustainable planet. The direct effect of such an effort in the form of a reduction in the emission of greenhouse gases and a reduction of the dependence on fossil fuels is motivated in [4], in which a battery swappable smart electric bus system is described that is currently in pilot operation. The performance study of electric buses in terms of actual measurements of range and energy consumption for some test city driving cycles is presented in [5]. A comparative economic analysis of different charging solutions for the range extension of systems, such as a trolley system, battery swapping and hybrid vehicles, is presented in [6,7].

Because of volume and especially the weight considerations, the amount of battery capacity used in a vehicle, such as a public transport bus, is limited, and consequently, the autonomous driving range of the bus is also limited. On some bus lines with limited driving distance per day, specific buses may have adequate range. However, more often, some sort of recharging of the batteries is necessary during the day. For medium and heavy use, recharging at a bus stop or at the turning point of the line (so-called opportunistic charging) may help enough to enable day-long operation.

For energy-intensive bus lines, like bus rapid transit with relatively high speed and high passenger occupancy, there is simply too little time available for getting the required energy into the bus with stationary solutions. In such scenarios, dynamic charging or battery swapping mechanisms need to be employed. Presently, several solutions are available to circumvent this problem.

- Trolley systems [6,7]: efficient energy transfer from overhead wires and a small, if any, energy buffer are needed. However, significant infrastructural costs are involved; mechanical contacts make the system inflexible and cause wear and tear, as well as cluttering of the landscape.
- Battery swapping [4,6]: the on-board battery is replaced at regular intervals at battery charging stations. The infrastructural costs and required battery capacity are high. While the transport efficiency is more due to a small on-board battery, the increase in required driving range leads to the increase in the number of battery swapping operations.
- Hybrid vehicles [6]: a combination of two or more energy sources are used. The design is complicated, and the vehicle cost is high. Transport efficiency decreases with the increase in on-board energy buffer weight.

An inductive power transfer (IPT) system for on-road EV charging is an upcoming option for driving range extension [8,9]. Wireless on-road charging systems for EVs can address several disadvantages associated with plugged-in vehicles related to safety, aesthetics and operational versatility in harsh weather conditions. Companies, like Bombardier Primove, Conductix Wamfler and Qualcomm Halo, are involved in pilot projects looking into the implementation of this technology. For example, Primove has successfully developed an electric route served by 12 m and 18 m e-buses with opportunity charging in Braunschweig, Germany [10]. During market research, the authors requested information on economic aspects from such companies. However, only ballpark figures were offered that were insufficient to carry out an independent viability study. Hence, the need was felt to develop a generalized economic viability study based on the technical knowledge [11,12].

The contribution of this paper is the development of a generalized economic viability study of employing a wireless on-road charging system for driving range extension. It is essential to describe how such dynamic charging systems measure up in terms of economics to other available charging solutions. However, since this technology is still in its nascent stage, historical data pertaining to

economic considerations of the system are scanty. A literature survey provides some ballpark figures, but these do not indicate the dependence on charging power level and road coverage. For example, the PATHteam [13] considers a baseline price assumption of 1.5 M€/km. The costs incurred for the on-line EV (OLEV) [14–16] for a 100 kW IPT system with four inverters/km and an I-type rail are estimated to be around 0.85 M$/km. Herein, the I-type rail refers to the structure of the magnetic core framework used in the rail at the primary side. A detailed analysis of the core structures used in the rails for shaping the magnetic fields is offered in [15]. In this, the cost estimate is given to be about 0.23 M$/km.

Economic viability, transport efficiency and initial infrastructural investment costs incurred are influenced by the charging power level of static and dynamic on-road charging, road coverage area and on-board battery capacity. This paper presents a detailed case-study on the economic considerations concerning the on-road wireless charging system for an articulated electric bus fleet in the province of North Holland. The theory is structured in a way that it can be adapted in a generalized economic viability study. In particular, the paper describes the choices designers must make in terms of static and dynamic charging power levels and the road coverage to develop the most economic on-road charging solution in order to achieve a given driving range and highlights the trends in incurred project cost by making specific choices. Further, the choice of on-board battery capacity based on the trade-off between savings due to efficient transport *versus* the extra incurred infrastructural costs for the IPT system is explored.

In Section 2, a generic methodology is developed to estimate the driving range extension due to different design parameters of the IPT system. A set of linear equations is defined that aids in analytically determining the battery state of charge (SoC) of an EV of any gross mass, frontal area, auxiliary power and for the charging power level and road coverage of a static and a dynamic IPT system. The defined equations can estimate the velocity-dependent energy consumption for EVs of any mass and frontal area irrespective of them being used in light, medium or heavy duty applications. Mass and area constants are determined to take into account the dependence of EV energy consumption on the velocity profile for several driving cycles. Further, the impact of battery weight on the SoC is incorporated in the equations.

Section 3 explores the economic aspects of a specific on-road charging system using the equations defined. Optimized design parameters with respect to P_{stat}, P_{dyn} and $C_{\text{road}}(\%)$ are presented for the case-study so as to minimize the cost incurred in installing the IPT system to achieve the required driving range. The theory developed in this document can be used for a generalized economic viability study of IPT systems for heavy duty EVs, such as e-buses. Underlying principles can also be adapted for other vehicle groups of varying mass and designs.

Section 4 looks into other factors, such as bus running schedule and on-board battery capacity, that may influence the lifetime cost incurred by the system. Particularly, the impact of increasing the possibility of opportunity charging during worst case scenario by increasing the scheduled stoppage time and the impact of reducing the battery weight as a trade-off between higher transport efficiency and higher infrastructural costs are explored.

2. Generic Methodology for Driving Range Estimation

In order to account for the energy inflow and outflow, it is essential to develop a model for the dynamic power consumption of the EV. This consumption pattern is dependent on the vehicle's specifications and the velocity profile. The dynamic power consumption is simulated for a reference vehicle with parameters [17] listed in Table 1.

Several standard driving cycles [18,19], like the standardised on-road test cycles (SORT 1, SORT 2 and SORT 3), the urban dynamometer driving schedule (UDDS), the Braunschweig cycle and the highway fuel economy driving schedule (HWFET), have been simulated to establish the methodology. The simulation results for the SORT 3 cycle are presented, and the "driving cycle constants" defined in the subsequent section are provided for all aforementioned driving cycles.

Table 1. Reference parameters for simulating the dynamical consumption model of the electric vehicle (EV).

Parameter	Value	Unit
Empty mass	13,300	kg
Gross mass	19,000	kg
Frontal area	8.568	m^2
Coefficient of drag (assumed)	0.7	-
Coefficient of rolling resistance (assumed)	0.01	-
Battery capacity	600 (200 × 3)	Ah
Energy capacity	324	kWh
Nominal voltage	540	V
Battery type	lithium ion	-
Initial state of charge (SoC) (assumed)	95%	-
Allowed depth of discharge (assumed)	80%	-

The physics of the vehicle power consumption [20] is governed by the following forces:

- Aerodynamic drag ($P_{\text{drag}} = 0.5\rho C_{\text{d}}|v|^3 A_{\text{f}}$) is the load due to resistance offered by the air. ρ is the density of air in kg/m^{-3}; C_{d} is the coefficient of drag; vis the instantaneous velocity; and A_{f} is the frontal area of the vehicle.
- Rolling resistance ($P_{\text{roll}} = C_{\text{r}} gM\cos(\theta)|v|$) is the frictional resistance offered by the road due to the motion of wheels. C_{r} is the coefficient of rolling resistance; M is the mass of the vehicle; g is the acceleration due to gravity; and θ is the angle of inclination.
- Inertial load ($P_{\text{I}} = Ma|v|$) is the change in the stored energy of the vehicle due to dynamic motion (acceleration/braking). It is important to consider here that some energy is recoverable through the regenerative braking.
- Gravitational load ($P_{\text{g}} = Mg\sin(\theta)|v|$) is due to the movement of the vehicle on an inclined road.

A dynamic power consumption model is developed based on the vehicle dynamics described by the above-mentioned equations depending on the power loss due to rolling resistance, power demand during acceleration, power lost during deceleration after, including regenerative braking, and power lost due to aerodynamic drag. The model involves the following assumptions:

- The overall average efficiency of the motor-drive system is assumed to be 80%. A corrective factor corresponding to the ratio of assumed average efficiency to actual average efficiency can be multiplied with the mass and area constant derived in the subsequent section to improve the accuracy of the model.
- Sixty percent of energy is recovered during regenerative braking.
- The angle of inclination of the road is zero.
- The auxiliary power P_{aux} will include heating, ventilation and air conditioning (HVAC), lighting, auxiliary services of vehicle, opening and closing of doors, route display screens, power steering and brakes. In the simulations to derive K_{m} and K_{a}, 0 kW is considered in order to eliminate the dependence of SoC on P_{aux}.
- Actual measurements were taken for the 12 m bus with a 324 kWh battery for SORT 1, 2 and 3 cycles. The specific consumption was measured to be 1.2 kWh/km for SORT 3 as compared to 1.3 kWh/km obtained from the simulation of our dynamic power consumption model under similar conditions. This increased the confidence on relying on the developed model for the economic viability study.

2.1. State of Charge Estimation of the Battery-Alone System

The impact of vehicle specifications, environmental factors and velocity profile on the SoC of the EV battery is simulated for a battery-alone system. Three Li-ion batteries are used in parallel (generic model available in matrix laboratory (MATLAB) software platform) with a nominal voltage of 540 V, a rated capacity of 200 Ah each and an initial SoC of 95%. Charge and discharge current flowing through this battery system are computed from the dynamic power flows and the nominal voltage of the system. The distance of 40 km is simulated to prove a linear dependence by regression analysis. A complete discharge of the battery up to the allowed depth of discharge (DoD) is not simulated for the regression analysis, implying that the dependence of internal battery resistance on the SoC is neglected in the derived constants of this section.

2.1.1. Mass Constant (K_m) of the Driving Cycle

Figure 1 shows the plots for SoC *versus* distance for different gross masses with the frontal area equal to zero and an ambient temperature of 20 °C for SORT 3 and the HWFET driving cycle. The auxiliary power demand of the EV is set to zero. The SoC, thus, in this case, depends only on the mass of the vehicle.

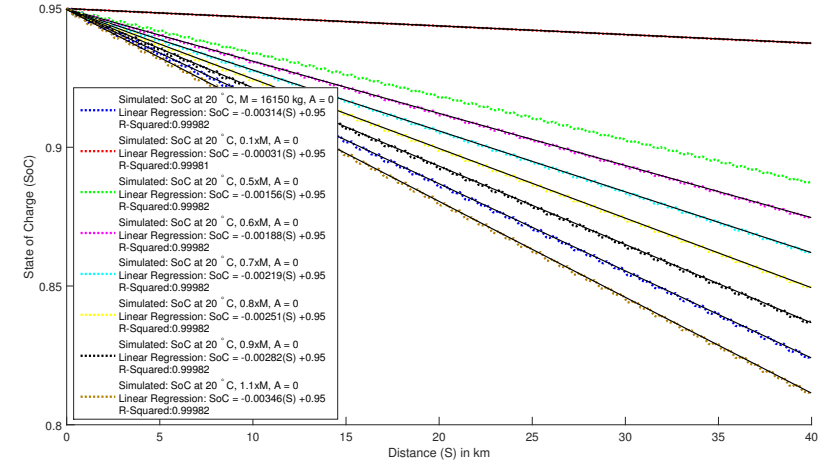

(**a**)

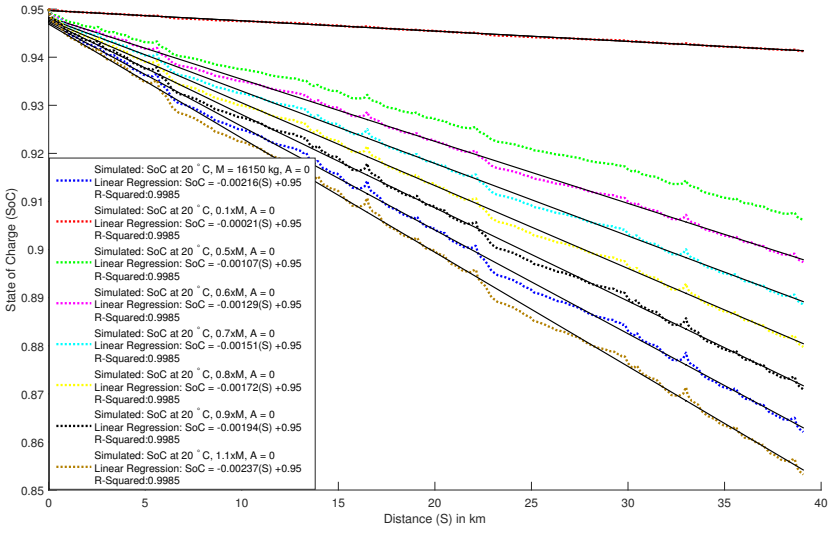

(**b**)

Figure 1. SoC *versus* distance for different gross masses of EV: (**a**) standardised on-road test cycle (SORT) 3 and (**b**) highway fuel economy driving schedule (HWFET).

The linear regression yields a coefficient of determination $(R^2) > 0.99$. An R^2 value close to one indicates a linear dependence of battery SoC on the distance traveled by the EV.

Figure 2 shows the variation of the slope of the SoC *vs.* distance with respect to mass of the vehicle for the SORT 3 and HWFET driving cycles. Regression analysis yields $R^2 > 0.99$, which indicates a linear dependence of final state of the charge of the battery on the vehicle mass. The slope, defined as the mass constant of the driving cycle K_m, is equal to 1.9464×10^{-7} for the SORT 3 driving cycle. In the case of the HWFET cycle, K_m is equal to 1.3371×10^{-7}.

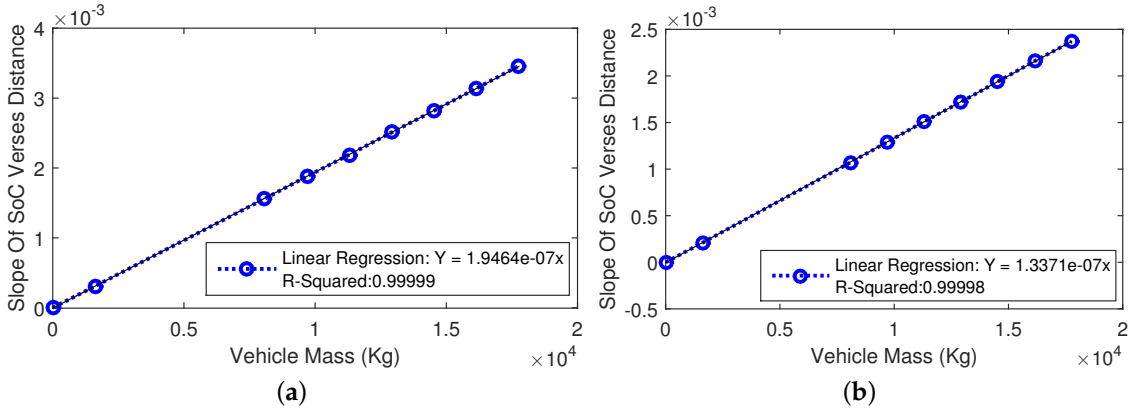

Figure 2. Slope of SoC *versus* distance w.r.t the gross mass of the vehicle: (**a**) SORT 3; and (**b**) HWFET.

2.1.2. Area Constant (K_a) of the Driving Cycle

Figure 3 shows the plots for SoC *versus* distance for different frontal areas with the gross mass equal to zero and an ambient temperature of 20 °C for the SORT 3 driving cycle. The auxiliary power demand of the EV is set to zero. The SoC, thus, in this case, depends only on the frontal area of the vehicle.

Figure 4 shows the variation of the slope of the SoC *vs.* distance with respect to the product of the frontal area and drag coefficient of the vehicle. The linear regression yields $R^2 > 0.99$, which indicates a linear dependence of the final battery SoC on the frontal area of the vehicle. The slope, defined as the area constant of the driving cycle, K_a=8.9739×10^{-5} for the SORT 3 driving cycle and 2.2176×10^{-4} for HWFET driving cycle.

2.1.3. Equation for State of Charge Estimation of the Battery-Only System

Hence, from the above theory, the expression for SoC of the on-board battery as a linear function of distance traveled can be derived. The SoC for the battery-alone EV system for any distance traveled can be estimated using Equation (1):

$$\mathrm{SoC_b} = -\left(\frac{K_m}{K_b}M + \frac{K_a}{K_b}A_f C_d + \frac{P_{aux}}{U_{av}\eta_{dis}E_{bat}}\right)S + \mathrm{SoC}(0) \quad (1)$$

A similar procedure was followed for different driving cycles to determine the velocity profile-dependent mass and area coefficients. Table 2 presents the mass and area constants of different driving cycles.

A clear increasing trend in area constant K_a with the average velocity of the driving cycle is observed, which is expected due to the increase in aerodynamic drag. On the other hand, the mass constant decreases despite increasing average velocity. This is because, while the mass-dependent vehicle power consumption is directly proportional to the instantaneous velocity, instantaneous power demand for acceleration is by far the dominant factor. Velocity profiles of driving cycles with

a lower average velocity typically have higher acceleration and deceleration durations, resulting in a higher power consumption. Thus, K_m decreases with the increase in average velocity.

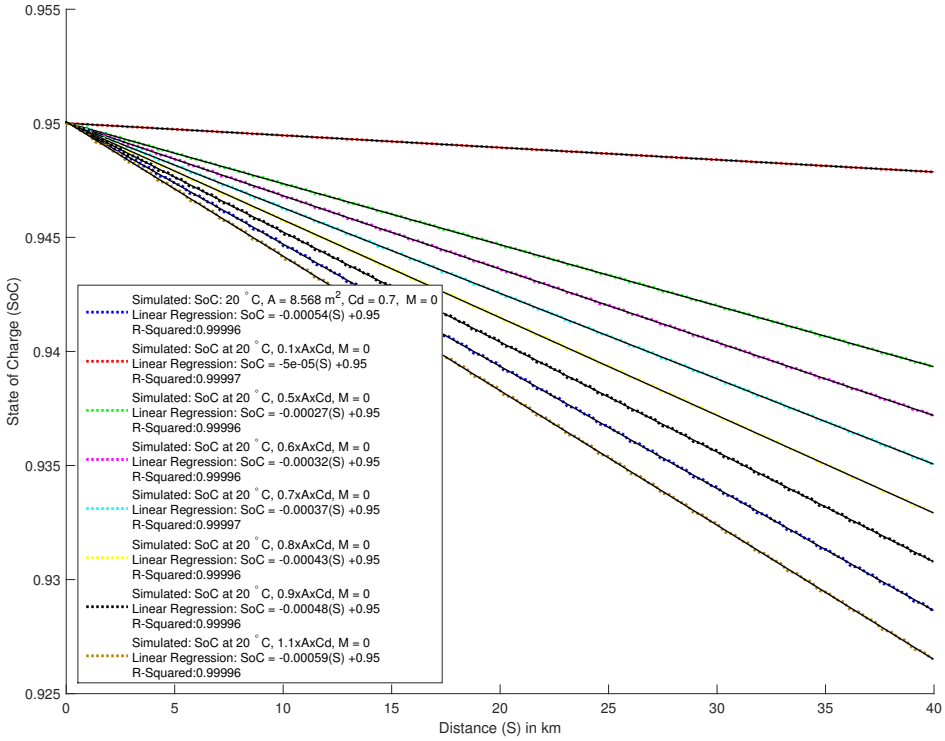

(**a**)

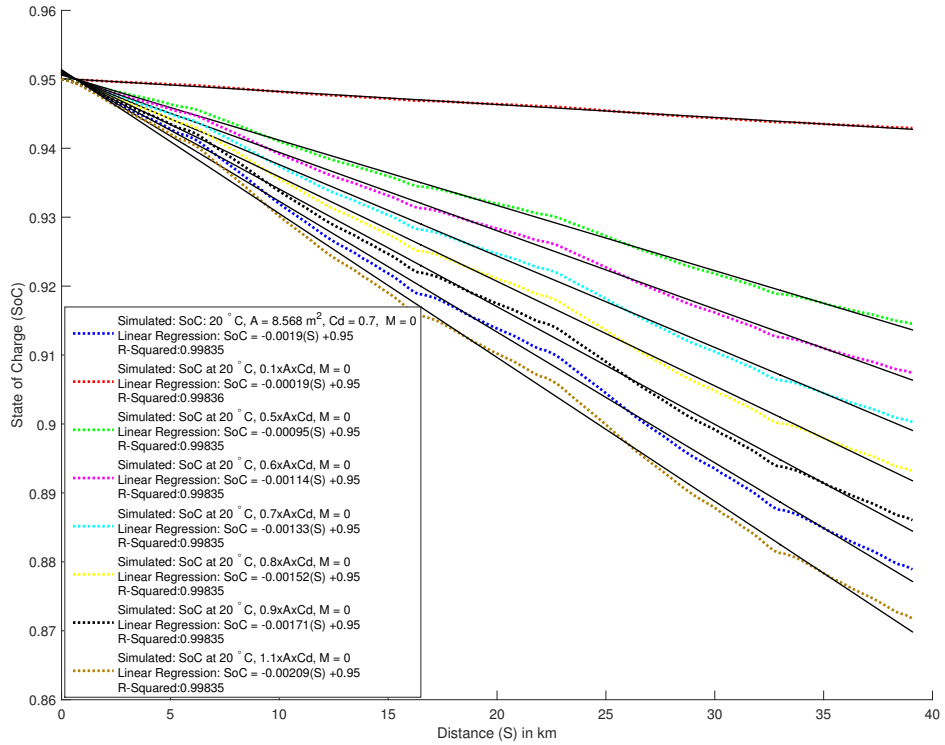

(**b**)

Figure 3. SoC *versus* distance for different frontal areas of the vehicle: (**a**) SORT 3; and (**b**) HWFET.

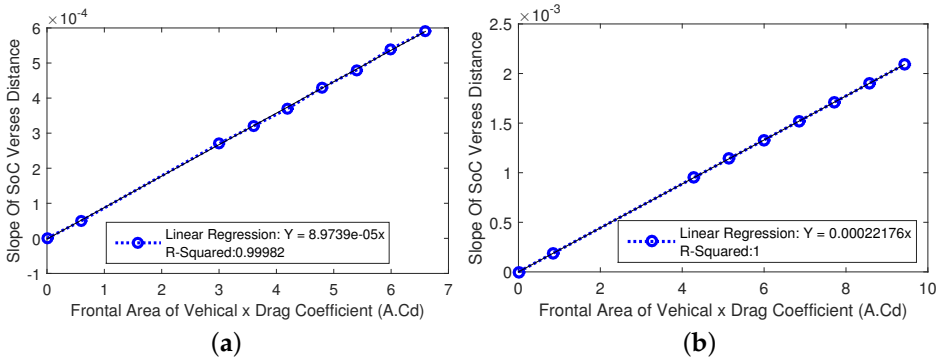

Figure 4. SoC *versus* distance for different frontal areas of the vehicle: (**a**) SORT 3; and (**b**) HWFET.

Table 2. Driving cycle constants. UDDS, Urban Dynamometer Driving Schedule.

Driving cycle	K_m (kg^{-1}km^{-1})	K_a (m^{-2}km^{-1})	U_{av} (km/h)
SORT 1	2.09234 ×10 $^{-7}$	2.4684 × 10^{-5}	12.1
SORT 2	1.9604 ×10^{-7}	4.9201 × 10^{-5}	18
Braunschweig	2.1225 ×10^{-7}	4.992 × 10^{-5}	22.9
SORT 3	1.9464 ×10^{-7}	8.9739 × 10^{-5}	25.3
UDDS	1.89 ×10^{-7}	9.3371 × 10^{-5}	31.53
HWFET	1.3371 ×10^{-7}	2.2176 × 10^{-4}	77.73

2.2. Driving Range Extension with the Static Inductive Power Transfer System

Static IPT charging is employed at scheduled stoppages of the driving cycle. For the same energy transfer per vehicle, the infrastructure cost involved in the static is less than the dynamic IPT system. The system is simulated with different static IPT charging power levels at scheduled stoppages of the SORT 3 driving cycle. Figure 5 shows the plots for the final battery SoC *versus* the power level for different scenarios for traveled distances of 40 km and 20 km.

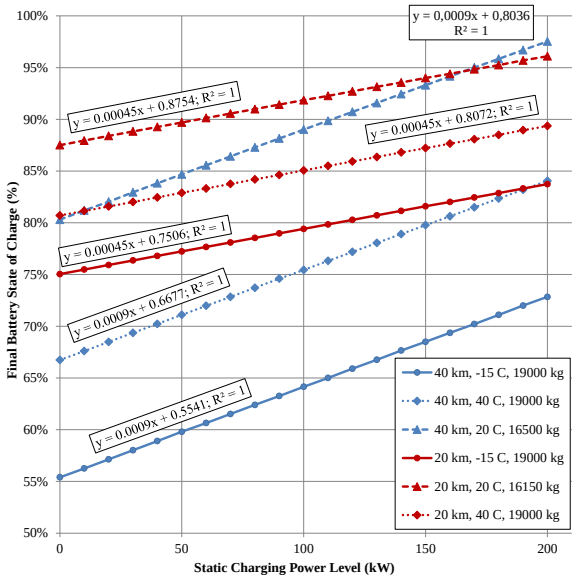

Figure 5. SoC of the battery for different charging powers of the static inductive power transfer (IPT) system.

The final SoC of the battery linearly varies with the charging power level. The regression analysis yields an R-squared value of one. The generic equation for estimating the SoC of the battery for different static charging power levels is described by Equation (2):

$$\mathrm{SoC}_{\mathrm{static}} = \left(\frac{t_{\mathrm{stop}} * \eta_{\mathrm{c}}}{E_{\mathrm{bat}}}\right) P_{\mathrm{stat}} + \mathrm{SoC}_{\mathrm{b}}(s_{\mathrm{tot}}) \tag{2}$$

The initial point $\mathrm{SoC}_{\mathrm{b}}(s_{\mathrm{tot}})$ is the SoC of the battery-alone system that can be estimated using Equation (1).

2.3. Driving Range Extension with the Dynamic Inductive Power Transfer System

Figure 6 shows the simulation plots for the final battery SoC *versus* the percentage of the road coverage area for different power levels of dynamic IPT charging for a traveled distance of 40 km with the SORT 3 driving cycle at an ambient temperature of −15 °C and 100% occupancy level. A static IPT system of 60 kW is considered to be installed in all cases.

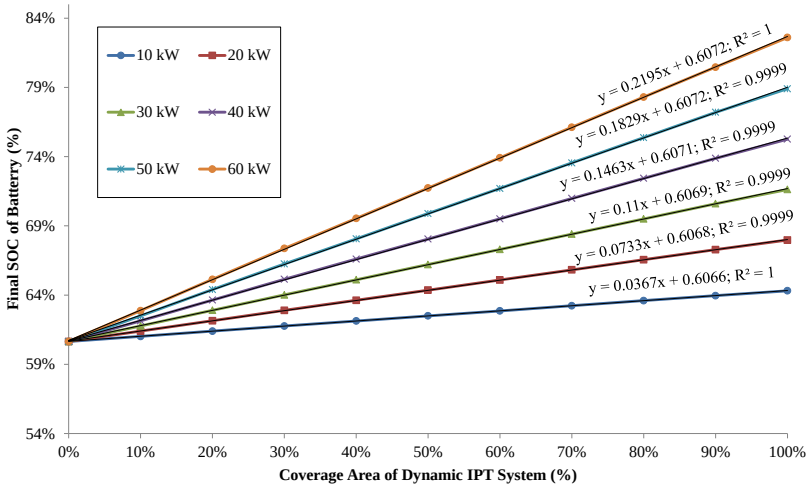

Figure 6. Final SoC *versus* road coverage area for different power levels of the dynamic IPT system.

The following observations can be made:

- The final SoC linearly increases with road coverage area despite the randomness in the velocity profile. This is because the IPT system is also randomly distributed on the road track. Regression analysis yields $R^2 > 0.99$, which indicates a strong correlation.
- The slope is directly proportional to the charging power level of the IPT system.
- SoC at the zero coverage area can be computed using Equations (1) and (2) corresponding to the "static-only" charging system.

The battery SoC of the EV with dynamic on-road charging can be estimated using Equation (3):

$$\mathrm{SoC}_{\mathrm{dyn}} = \mathrm{SoC}_{\mathrm{static}} + \underbrace{\left(\frac{(t_{\mathrm{total}} - t_{\mathrm{stop}})\eta_{\mathrm{c}} P_{\mathrm{dyn}}}{E_{\mathrm{bat}}}\right)}_{\mathrm{Slope}} \frac{(C_{\mathrm{road}}(\%))}{100} \tag{3}$$

The driving range of the vehicle can be calculated from the SoC of the battery using Equation (4):

$$DR = \frac{(DoD_{\max} \times S)}{(\mathrm{SoC}(0) - \mathrm{SoC}_{\mathrm{final}})} \tag{4}$$

2.4. Impact of Battery Weight

In the previous section, the impact of IPT systems on the driving range of the EV was studied. In order to achieve the same driving range with the battery-alone system, a greater energy capacity is needed and, hence, a greater battery weight and volume, which has implications on not only the transport efficiency [22], but also on the feasibility of installing such a system. This section describes the method to estimate the required energy capacity of the battery in order to achieve the desired driving range and the subsequent impact of increased weight on specific consumption of the electric bus.

Rearranging Equation (4), the final SoC of the battery (SoC_{req}) for the required driving range at the end of travel distance is described by Equation (5):

$$SoC_{req} = SoC(0) - \frac{DoD_{max} * S}{DR} \tag{5}$$

Here, DR is the required driving range in km. Now, Equation (1) can be modified to compute the battery weight-dependent SoC at end of the total traveled distance, as shown in Equation (6):

$$SoC_b = -\left(\frac{K_m}{K_b}(M_{ref} - W_{bat,ref}(1-k_b)) + \frac{K_a}{K_b}A_f C_d + \frac{P_{aux}}{U_{av}\eta_{dis}k_b E_{bat,ref}}\right)S + SoC(0) \tag{6}$$

where M_{ref} is the gross mass of the reference vehicle and $W_{bat,ref}$ is the weight of the reference vehicle battery in kg. The weight of the required battery is $K_b W_{bat,ref}$. Rearranging Equation (6), it is possible to estimate the required battery capacity factor K_b as per Equation (7), such that the SoC_{final} corresponding to the required driving range is equal to SoC_b for a battery-alone system.

$$K_b = \frac{K_m(M_{ref} - W_{bat,ref}) + K_a A_f C_d + \left(\frac{P_{aux}}{U_{av}\eta_{dis}E_{bat,ref}}\right)}{\left(\frac{SoC(0)-SoC_{ref}}{S}\right) - K_m W_{bat,ref}} \tag{7}$$

From the Ragone plot, the specific energy of a high-power Li-ion battery used in the reference e-bus is about 100 Wh/kg [23]. Hence, the weight of the reference vehicle ($W_{bat,ref}$) is $\left(\frac{1000*E_{bat,ref}}{100}\right) = 3240$ kg. Figure 7 shows the increase in the capacity factor and the specific consumption of the electric bus with the required driving range for different loading scenarios for the SORT 3 driving cycle for the battery-alone system with no on-road charging in place. The simulated specific consumption of the reference electric bus used in this section is also marked.

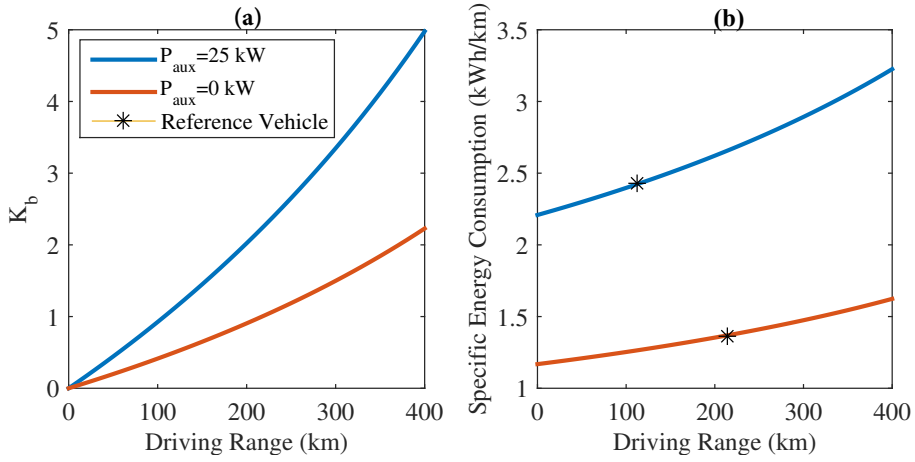

Figure 7. Impact of driving range of the vehicle for the SORT 3 driving cycle without any on-road charging on the (**a**) capacity factor K_b (**b**) specific consumption.

Finally, the impact of the increase in the battery weight on the specific consumption of the vehicle ($E_{specific}$ in kWh/km) can be estimated from Equation (8):

$$E_{specific} = E_{bat} * \left(K_m(M_{ref} - W_{bat,ref}(1 - K_b)) + K_a A_f C_d + \frac{P_{aux}}{U_{av}\eta_{dis}E_{bat,ref}} \right) \quad (8)$$

2.5. Estimation Error

In Figure 8, the percentage of absolute error between the estimated value obtained from the derived equations and the simulated value of the battery SoC of the reference vehicle obtained from the dynamic power consumption model of the vehicle developed on MATLAB for a 40 km traveled distance with 60 kW static + 60 kW dynamic on-road charging is presented for different driving cycles.

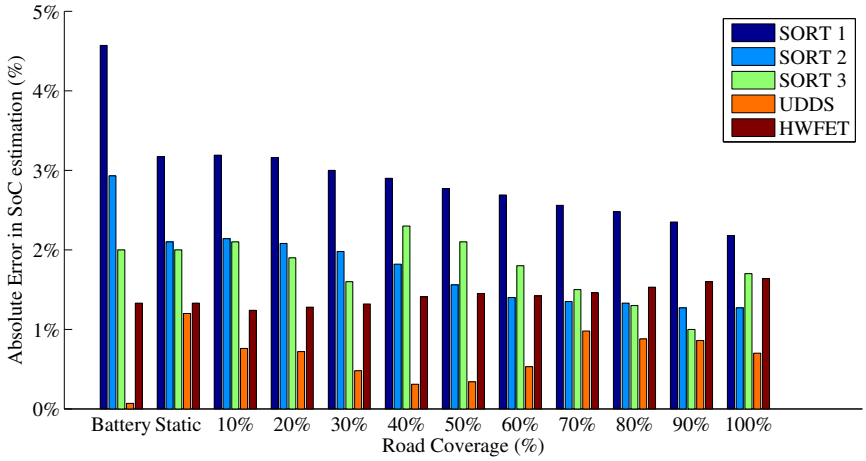

Figure 8. Percentage of the absolute error in SoC estimation for different driving cycles.

For a 30% road coverage with 60 kW charging power level of both the static and dynamic IPT system, the error in estimated SoC is 2% with the corresponding error in estimated driving range being 6.69%. Hence, the driving range of any EV in different scenarios can be estimated using simple linear equations with known parameters and vehicle specifications with reasonable accuracy.

3. Economic Analysis for the On-Road Inductive Power Transfer Charging System: Case Study

3.1. System Description

The economic aspects of on-road charging solution for a two-lane, 40 km-long bus line of Zuidtangent in the province of North Holland is explored. It should be noted that in this section, a larger articulated electric bus will be used for analysis with an empty weight of 20,000 kg and a 500 kWh on-board Li-ion battery pack with an additional weight of 5000 kg. The gross weight of the vehicle with 100% occupancy level is thus about 35,000 kg. The frontal area is 8.568 m^2; the coefficient of drag is taken as 0.7; and the rolling resistance is taken as 0.01. Twenty five articulated buses run per day on average. Each bus is expected to drive 400 km per day. Five buses are kept as spare. The design of the IPT system involves the following considerations:

- The battery is charged to its full capacity during night hours when the bus is stationary.
- There are 24 scheduled stoppages of 20 s each and a 6 min stoppage at the start of each run.
- The UDDS [19] is used to emulate the velocity profile of the e-bus.
  - The average velocity of the UDDS driving cycle is 31.53 km/h.
  - From Table 2, the mass constant is 1.89 $\times$ 10 $^{-7}$, and the area constant is 9.337 $\times$ 10 $^{-5}$.

- The required driving range is 400 km (10 trips of 40 km each) in the worst case scenario of −15 °C, 100% occupancy.
- The climate model in [21] predicts that a normal bus would consume 167 kWh for HVAC in winter days for −7 °C in Netherlands for a 20 h operation. An articulated bus of almost double the length would consume double this (334 kWh). Correspondingly, 433 kWh will be consumed if the ambient temperature is −15 °C.

  The total energy consumption of the auxiliary system, including HVAC, lighting, auxiliary services of the vehicle, opening and closing of doors, route display screens, power steering and brakes, during the worst winter condition is assumed to be 500 kWh for a 20 h operation. Therefore, the average P_{aux} is assumed to be 25 kW.

The SoC for the battery-alone system can be estimated from Equation (1). With an initial SoC of 95% at the start of the day by considering overnight charging of the on-board battery of the electric bus, the SoC at the end of a 40 km travel distance without any on-road charging is 68.66%. At the end of the traveled distance (S = 40 km), the final SoC of the battery corresponding to the desired driving range (DR = 400 km) is given by Equation (5) to be 87%. The deficit, ΔSoC = 18.34%, is removed using a combination of static and dynamic on-road charging.

P_{stat}, P_{dyn} and $C_{road}(\%)$ are varied, such that SoC_{dyn} at the end of traveled distance of 40 km is 87%. Several combinations can be used to achieve the required driving range, and the optimum values are chosen based on the minimum investment costs involved.

3.2. ΔSoC Deficit Removal with the Static Inductive Power Transfer Charging System

Static charging pads are installed at the scheduled stoppages. The charging time with each pad is 20 s. For a similar amount of charging time on a single dynamic IPT segment of 1.05 m, the e-bus must have a velocity of 0.19 kmph. Hence, for better infrastructural usage and lower investment costs, it is desirable that the static charging power be as high as possible.

The slope of Equation (2) corresponding to the stop time in the winter worst case scenario is 0.000453. Figure 9 shows the variation in final battery SoC and driving range achieved for different on-road static charging power levels for different starting and halt times. Note that with increasing halt time, the total daily operating time of the bus increases, thereby marginally increasing the energy consumption of the auxiliary bus system. This is reflected in decreasing SoC of Equation (1) due to decreasing average velocity (U_{av}).

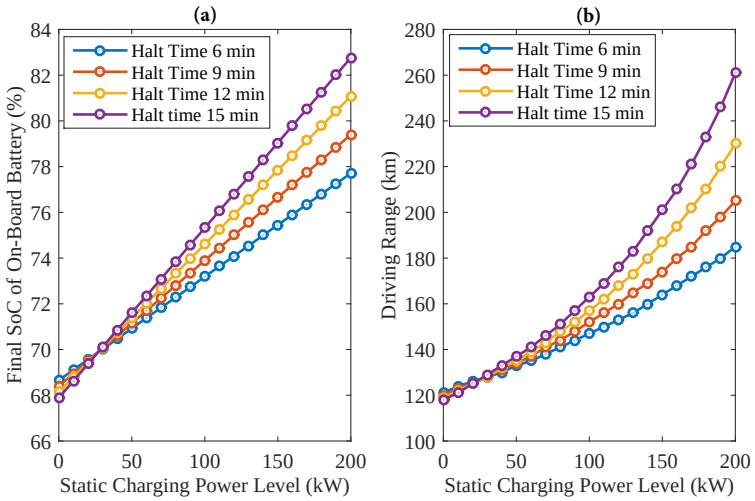

Figure 9. (**a**) On-board battery SoC (**b**) driving range *versus* static charging power level for different starting and halt times.

With a 200 kW static charging power level, the driving range achieved is 185 km, and the battery SoC is 77.7%. The deficit has to be cleared by installing dynamic charging infrastructure.

3.3. ΔSoC Deficit Removal with the Dynamic Inductive Power Transfer Charging System

With increasing power level, the percentage of road coverage to achieve the required driving range of 400 km decreases; however, the investment costs per km of installed on-road charging infrastructure increases, as shown in Figure 10.

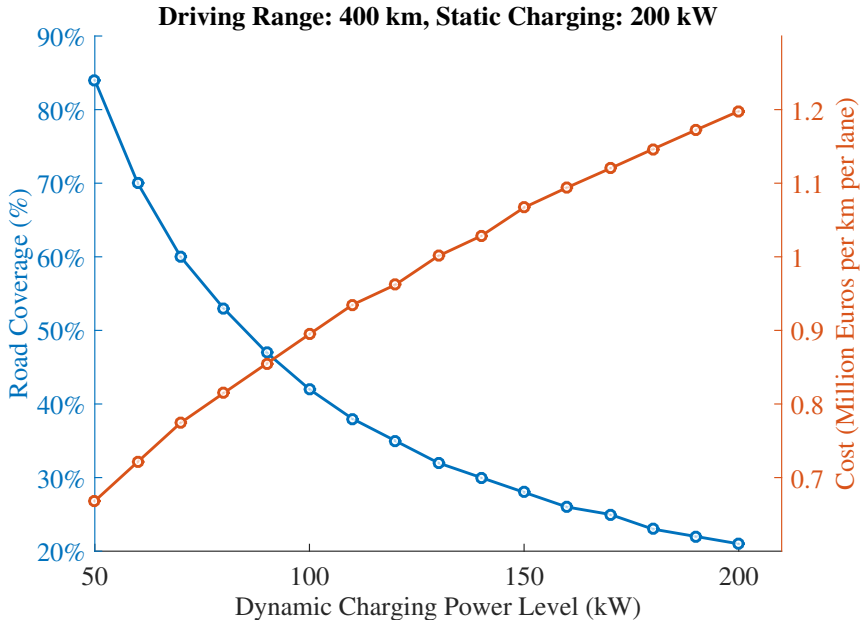

Figure 10. Percentage of road coverage for different dynamic charging power levels.

As shall be shown in the subsequent section, the investment costs incurred due to increasing the charging power level are outmatched by the decrease in infrastructural costs due to reducing road coverage. Hence, it is preferred to increase the charging power level from the economic point of view.

3.4. Cost of System Components

In this section, the investment costs incurred for different system components have been estimated. Since the technology is still in its nascent stage, market data are not available. Hence, the costs have been calculated from the design point of view. The following considerations have been observed to make the estimate:

- The total copper mass (in kg) in the air cored primary winding [24] based on the charging power level along with Litz wire cost [25] of 35 €/kg are used to estimate the cost of a single IPT charging pad. An additional design cost of 50% is assumed.
- The cost of the power electronics [26] involved in the IPT supply system is considered to be 50 €/kW. Additional maintenance charges of 10% have been included.
- Corresponding to the operating frequency of 100 kHz, a minimum of 4 inverters per km are installed [27].
- The road construction (digging, labor, installation of IPT system) costs of 0.1 M€/km for IPT road coverage are assumed.
- Discrete charging pads of 1.05 m [24] in length each have been considered for dynamic on-road charging. The total number of dynamic charging pads have been estimated for total road coverage, and the corresponding cost of air cored primary winding is calculated. An illustration of the on-road dynamic charging system with discrete pads [28] is shown in Figure 11.

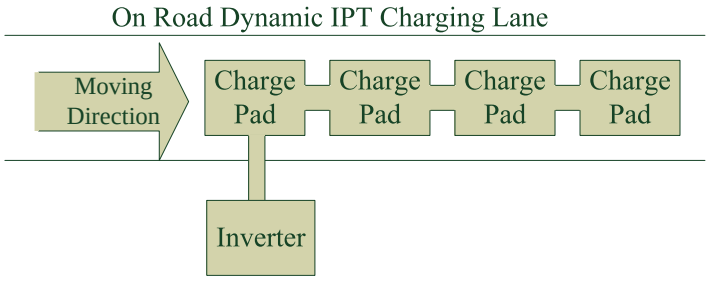

Figure 11. Illustration of the discrete IPT charging pads for on-road dynamic charging.

Figure 12 shows the total cost of different IPT system components for achieving a driving range of 400 km with a 200 kW static IPT charging at scheduled stoppages and different dynamic charging power levels. The overall cost incurred decreases with increasing dynamic charging power level, because of the decrease in the percentage of road coverage. With a 200 kW dynamic charging, the total road coverage required is 21%, while the IPT system cost is 10.1 million Euros per lane of the Zuidtangent line. The specific cost is 1.2 M€/km/lane.

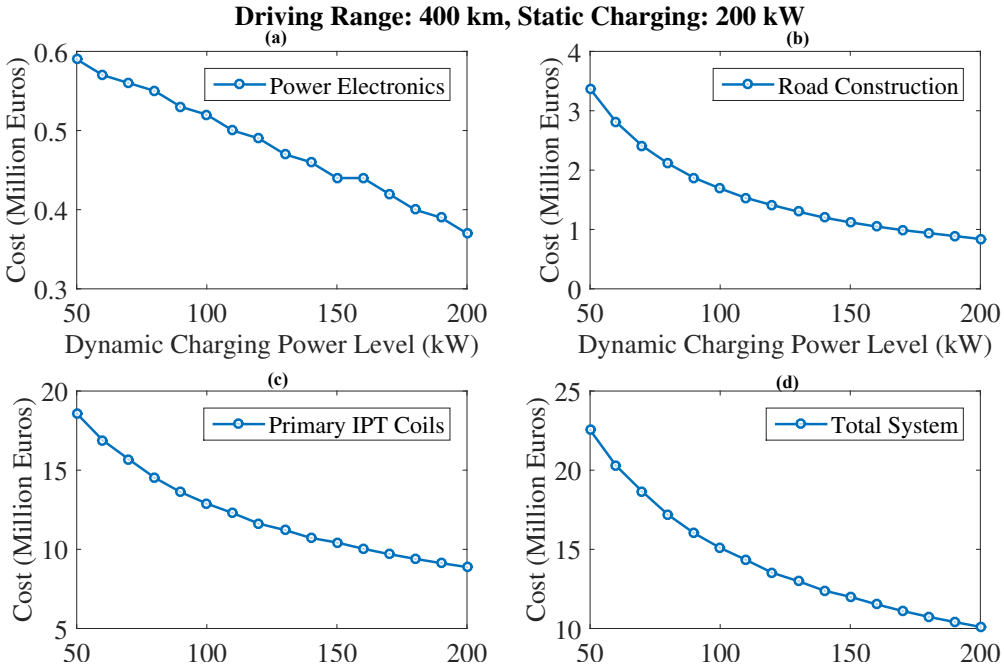

Figure 12. Cost estimation of the IPT charging system components (**a**) power electronics (**b**) road contruction; (**c**) primary IPT coils; and (**d**) total system.

4. Second Order Economic Considerations

Several secondary factors influence the choice of system configuration. These include the following.

4.1. Running Schedule

In the beginning of each 40 km run, there is a six min scheduled stop that provides an opportunity for static charging. During the worst loading scenario, which occurs only for a few predictable days of a year, increasing this stoppage time can lead to significant infrastructural cost reduction for meeting the driving range. Extra buses may be employed to run in these conditions for meeting the time deficit. Note that with increasing halt time, the total daily operating time of the bus

increases, thereby marginally increasing the energy consumption of the auxiliary bus system. This is reflected in the decreasing SoC of Equation (1) due to decreasing average velocity (U_{av}).

Figure 13 shows the influence of scheduled stoppage time at the start of the 40 km run on the incurred investment cost of installing the IPT system for different battery capacities.

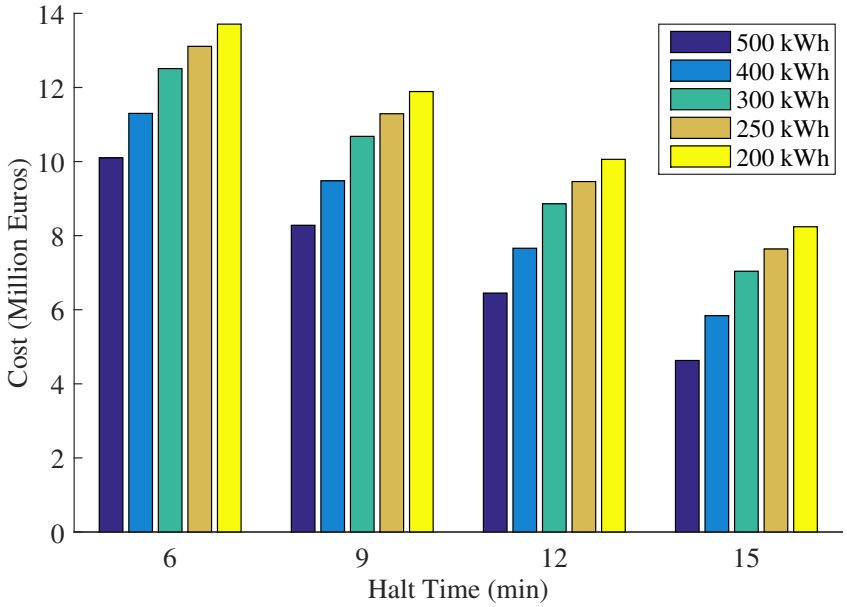

Figure 13. Incurred IPT infrastructure cost with changing halt time at the start of the 40 km run.

As observed, the incurred investment costs of installing on-road charging infrastructure significantly decreases by increasing the halt time. Hence, by choosing a halt time of 12 min during the worst loading scenario, the IPT system cost decreases from 10.1 M€/lane to 6.45 M€/lane, because the required road coverage of dynamic on-road charging decreases from 21% to 13%.

4.2. On-Board Battery Capacity

- The transport efficiency increases with decreasing battery capacity corresponding to the weight reduction. The energy savings becomes significant with a high lifetime travel distance and the number of running buses.
- IPT charging infrastructure cost increases with decreasing battery capacity due to the additional road coverage requirement of the dynamic IPT system. This is shown in Figure 13.
- The price of the installed on-board battery decreases with decreasing capacity. This can be a significant investment factor with increasing the number of e-buses.

Figure 14 shows the IPT charging infrastructure cost, on-board battery cost and the total project cost for a 25 average running +5 spare all-electric bus system with decreasing battery size. Recall here that the charging power delivered to the on-board battery by the IPT system is 200 kW. Both static charging at scheduled stoppages, as well as dynamic charging with 13% road coverage are employed to obtain a driving range of 400 km.

The Li-ion battery price is considered to be 700 €/kWh and can last for about 12 years before needing replacement [6]. This relatively high price level is caused by high quality requirements and limited market size for buses so far. In five to 10 years, the cost is predicted to drop to approximately 250 €/kWh [29].

The total incurred project investment cost slightly increases with decreasing battery size as a net effect of the increase in IPT infrastructure cost balanced by the decrease in total battery cost. For attaining higher transport efficiency, it is desirable that the on-board battery capacity is lower. Hence there is a trade-off in selecting the on-board battery capacity, which is now explored.

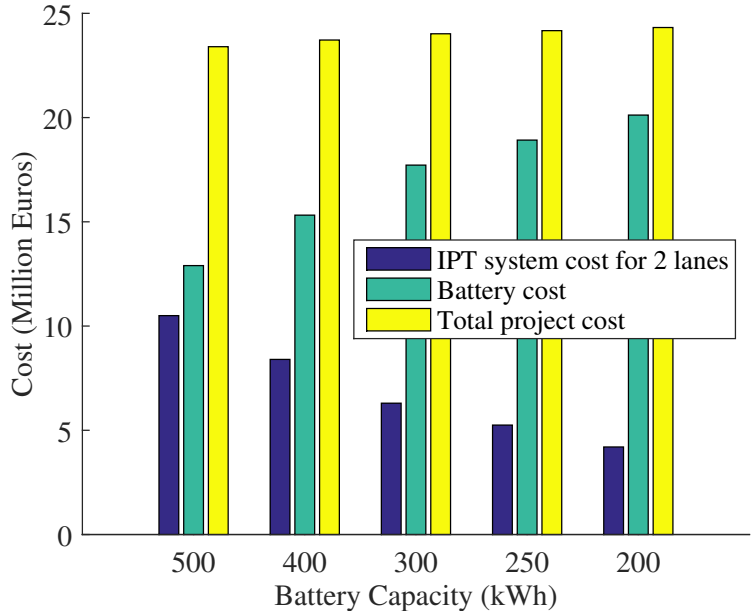

Figure 14. Battery size dependency of the incurred infrastructural costs.

The OLEV team looks into the trade-off between battery capacity, transport efficiency and charging infrastructural costs by defining the optimization problem [30] using particle swarm optimization based on the system dynamics. The solution involves allocating power transmitters to determine battery size by minimizing the vehicle power consumption while constrained by the battery energy level to be maintained.

In this paper, the derived linear equations reduce the optimization problem to a solution of two linear equations with known constants without dynamic terms, as shown in Figure 15, as against optimization techniques used in prior literature [31]. The optimum solution can be reached quickly by solving for the savings based on the specific energy consumption using Equation (8) with the single variable "K_b" that describes the battery capacity against the incurred minimum infrastructural costs for the desired driving range for that K_b, as described in the above sections.

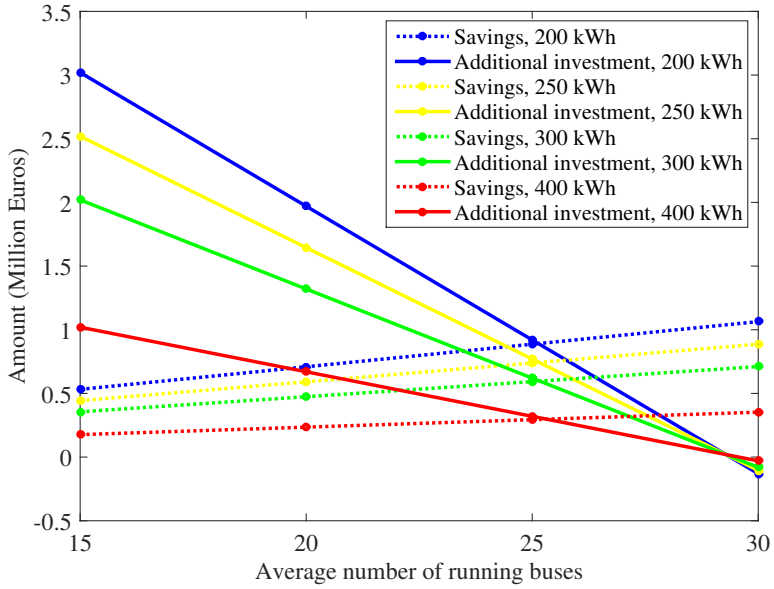

Figure 15. Savings and change in initial investment for different battery sizes with respect to a 500 kWh on-board battery system.

From Equation (8), the specific consumption of the electric bus in the average loading scenario (25 kW of auxiliary power consumption and 100% occupancy level) is estimated to be 2.84 kWh/km with a 500 kWh on-board battery and 2.66 kWh/km with a 200 kWh on-board battery with a battery-specific weight of 10 kg/kWh.

Savings achieved in 12 years of operation due to efficient transport with varying kWh on-board batteries for different average numbers of running buses is shown in Figure 15. Ten percent additional losses corresponding to the IPT system transfer efficiency are assumed. Energy cost is considered to be 0.1 €/kWh, and each bus runs for an average of 400 km per day. The change in investment corresponding to the net effect of the increase in the IPT infrastructure cost and the decrease in the total on-board battery cost ("x" running buses) is also depicted.

Figure 15 shows that the reduction of the on-board battery size from 500 kWh to 200 kWh is only viable if an average of 30 buses are running daily. The point of intersection of the savings trend and the extra infrastructure trend (same colored lines) gives the average number of buses running per day above which a reduction in the on-board battery capacity becomes a viable option. In our system (25 buses running on average per day), the extra incurred costs cannot be recovered by efficient transport in a 12 year lifetime for even a 500 kWh to 400 kWh battery size reduction. Hence, we conclude that 500 kWh is cost-wise the most optimum choice.

5. Conclusions

Hence, the economic analysis of installing the IPT system to achieve a driving range of 400 km in the worst loading scenario on the Zuidtangent bus lanein the province of North Holland was carried out. Table 3 summarizes the IPT system parameters in terms of the charging power level (200 kW), road coverage percentage (13%), inverter rating (200 kW) and battery capacity (500 kWh) for the system described. The resulting specific cost is estimated to be 1.2 M€/km/lane for a lifetime of 12 years.

In order to develop a generalized theory towards this study, an analytical methodology has been presented to estimate the extension in driving range of any EV with on-road contactless charging. The SoC of the battery is described as a linear function of the distance traveled and can be estimated for an EV of any gross mass and frontal area. The energy consumption dependent on the velocity profile is estimated by defining mass and area constants for several driving cycles. The increase in the SoC of the battery depending on different power levels and road coverage of the static and dynamic IPT system is described mathematically.

The presented theory describes how to minimize the infrastructural costs based on the IPT design parameters. The paper depicts how the infrastructural costs of dynamic wireless charging systems decrease with increasing power level due to the reduction in road coverage area and, hence, suggests to the designers to realize as high a charging power as possible. Further, the scheduled stoppage time is increased during the worst weather/load conditions to achieve a more economically-viable system. This solution brings down the cost from 10.1 M€/lane to 6.45 M€/lane due to a reduction in road coverage of dynamic charging from 21% to 13%.

Another major contribution of this publication is the optimization of on-board battery capacity as a trade-off between the savings achieved due to the increase in transport efficiency and the extra investment costs incurred due to the battery weight reduction. The derived linear equations in this paper reduce the optimization problem to a solution of two linear equations with known constants. It is also shown how a 500 kWh on-board battery capacity is chosen as the most optimized option. It is depicted how increasing the number of average running buses in the system can make the battery weight reduction a viable option.

The so-called lifetime impact (including fabrication, use and scrappage) of an EV in terms of CO_2 emission is dependent on the source of electric energy. If the electricity used is purely from coal-fired power plants, there is only a limited reduction in overall CO_2 emissions compared to a diesel-fueled vehicle of identical proportions. If more sustainable sources are added to the electricity generation

mix (partly from renewables, partly natural gas, *etc*., as is often the case), there is a clear reduction in lifetime CO_2 impact for the EV compared to the diesel-based vehicles [32].

Table 3. IPT system specifications.

Parameter	Value	Unit
On-board battery capacity	500	kWh
Driving range in worst loading scenario	400	km
Driving range without on-road charging	119	km
Scheduled stoppage at start of each run (worst case)	12	min
Scheduled stoppage at start of each run (normal)	6	min
Number of buses (average running + spare)	25 + 5	-
Static charging power level	200	kW
Dynamic charging power level	200	kW
Dynamic IPT road coverage	13%	-
Power rating of inverter	200	kW
Total number of inverters	22	-
Cost of primary winding	5.67	M€/lane
Cost of inverters	0.24	M€/lane
Total cost of IPT system	6.45	M€/lane
Specific cost	1.2	M€/km/lane
Battery cost for 30 buses	10.5	M€
Total project cost (M€/2 lanes/30 buses)	23.4	-

While IPT on-road charging of electric buses might offer an advantage over hybrid or completely diesel-based vehicles in terms of CO_2 emission reduction, another research objective was to utilize this cost analysis as a comparative tool to evaluate how IPT charging systems measure up to other solutions for extending the driving range of such electric buses in terms of economics [7]. At present, the specific cost of 1.2 M€/km/lane for this system is higher as compared to 0.75 M€/km/lane of a conventional trolley system. However, it must be noted that a conservative battery price of €700/km is taken, which is expected to decrease with the future evolution of market forces in favor of such technologies.

Acknowledgments: The authors wish to acknowledge Ir. Mark Leendertse for providing the design image of the future mobility vision of DCE& S group of TU Delft used for the illustration of this document and the Province of North Holland, by whose order the study on electrification of R-300 bus route was initiated.

Author Contributions: Aditya Shekhar was the primary investigator who developed the simulation models, defined the generic equations and carried out the economic analysis study. Venugopal Prasanth shared his experience and knowledge in inductive power transfer technology. He looked into the design of the wireless charging system that aided in the economic analysis study. Pavol Bauer and Mark Bolech were responsible for the design of the study. They provided information on pricing of various system components and defined the system requirements on which the study was based.

Conflicts of Interest: The authors declare no conflict of interest.

Nomenclature

SoC_b	SoC of battery at the end of the traveled distance
$SoC(0)$	Initial SoC of the battery
S	Total distance traveled by the vehicle in km
K_m	Mass constant of the driving cycle in $kg^{-1}km^{-1}$
M	Gross mass of the vehicle in kg
K_a	Area constant of the driving cycle in $m^{-2}km^{-1}$
A_f	Frontal area of the vehicle in m^2
C_d	Coefficient of drag
P_{aux}	Power demand of the auxiliary system of the vehicle in kW
U_{av}	Average velocity in km/h
η_{dis}	Discharge efficiency of the battery
E_{bat}	Energy capacity of vehicle battery in kWh
K_b	Capacity factor defined as the ratio of the maximum energy that can be delivered by the EV battery to the maximum energy that can be delivered by the reference battery $\left(=\frac{\eta_{dis}E_{bat}}{\eta_{dis,ref}E_{bat,ref}}\right)$
SoC_{static}	SoC of battery at the end of traveled distance with a static charging system
t_{stop}	Total scheduled stoppage time spent on the IPT charging system in hours
η_c	Charging efficiency of the battery
P_{stat}	Static IPT charging power level in kW
$SoC_b(s_{tot})$	SoC at the end of the total traveled distance without any on-road charging
SoC_{dyn}	State of the charge of the battery at the end of traveled distance
t_{total}	Total travel time in hours
P_{dyn}	Dynamic charging power level in kW
$C_{road}(\%)$	% Road coverage of dynamic IPT
DR	Driving range in km
DoD_{max}	Maximum allowed depth of discharge, assumed to be 80%.

References

1. Fox, G.H. Electric Vehicle Charging Stations: Are We Prepared? *Ind. Appl. Mag.* **2013**, *19*, 32–38.
2. Maheshwari, P.; Tambawala, Y.; Nunna, H.S.V.S.K.; Doolla, S. A review on plug-in electric vehicles charging: Standards and impact on distribution system. In Proceedings of the 2014 IEEE International Conference on Power Electronics, Drives and Energy Systems (PEDES), Mumbai, India, 16–19 December 2014; pp. 1–6.
3. Mwasilu, F.; Justo, J.J.; Kim, E.-K.; Do, T.D.; Jung, J.-W. Electric vehicles and smart grid interaction: A review on vehicle to grid and renewable energy sources integration. *Renew. Sustain. Energy Rev.* **2014**, *34*, 501–516.
4. Choi, W.; Kim, J. Electrification of public transportation: Battery swappable smart electric bus with battery swapping station. In Proceedings of the 2014 IEEE Conference and Expo, Transportation Electrification Asia-Pacific (ITEC Asia-Pacific), Beijing, China, 31 August–3 September 2014; pp. 1–8.
5. *Performance of Electric Buses in Practice: Energy Consumption and Range*; TNO Report 2013 R10212; The Netherlands Organisation for Applied Scientific Research (TNO): Delft, The Netherlands, 2013.
6. *E-Buses for SolaRoad*; *TNO Report for the Province of North Holland*; The Netherlands Organisation for Applied Scientific Research (TNO): Delft, The Netherlands, 2014.
7. *Electric Buses for SolaRoad II*; *Internal TNO Document 2015 R10055*; The Netherlands Organisation for Applied Scientific Research (TNO): Delft, The Netherlands, 2015.
8. Wu, H.H.; Gilchrist, A.; Sealy, K.; Israelsen, P.; Muhs, J. A review on inductive charging for electric vehicles. In Proceedings of the 2011 IEEE International Electric Machines & Drives Conference (IEMDC), Niagara Falls, ON, Canada, 15–18 May 2011; pp. 143–147.
9. Prasanth, V.; Bauer, P. Distributed IPT Systems for Dynamic Powering: Misalignment Analysis. *IEEE Trans. Ind. Electron.* **2014**, *61*, 6013–6021.
10. Bombardier PRIMOVE Website. Available online: http://primove.bombardier.com/media/news/ (accessed on 15 October 2015).
11. Shekhar, A.; Prasanth, V.; Bauer, P.; Bolech, M. Generic methodology for driving range estimation of electric vehicle with on-road charging. In Proceedings of the 2015 IEEE Transportation Electrification Conference and Expo (ITEC), Dearborn, MI, USA, 14–17 June 2015; pp. 1–8.

12. Shekhar, A.; Bolech, M.; Prasanth, V.; Bauer, P. Economic considerations for on-road wireless charging systems—A case study. In Proceedings of the 2015 IEEE PELS Workshop on Emerging Technologies: Wireless Power (WoW), Daejeon, Korea, 5–6 June 2015; pp. 1–5.
13. *Roadway Powered Electric Vehicle Project Parametric Studies: Phase 3D Final Report*; *California Partners for Advanced Transit and Highways Research Report*; University of California: Berkeley, CA, USA, 1996.
14. Jang, Y.J.; Suh, E.S.; Kim, J.W. System Architecture and Mathematical Models of Electric Transit Bus System Utilizing Wireless Power Transfer Technology. *IEEE Syst. J.* **2015**, doi:10.1109/JSYST.2014.2369485.
15. Shin, J.; Shin, S.; Kim, Y.; Ahn, S.; Lee, S.; Jung, G.; Jeon, S.-J.; Cho, D.-H. Design and Implementation of Shaped Magnetic-Resonance-Based Wireless Power Transfer System for Roadway-Powered Moving Electric Vehicles. *IEEE Trans. Ind. Electron.* **2014**, *61*, 1179–1192.
16. Rim, C.T. The Development and Deployment of On-Line Electric Vehicle (OLEV). In Proceedings of the IEEE Energy Conversion Congress and Exposition (ECCE), Denver, CO, USA, 15–19 September 2013.
17. Build Your Dreams (BYD) E-Bus. 2014. Available online: http://www.byd.com/la/auto/ebus.html (accessed on 13 September 2014).
18. *Standardised On-Road Test Cycles*; International Association of Public Transport (UITP): Brussels, Belgium, 2009.
19. United States Environmental Protection Agency. Dynamometer Drive Schedules. Available online: http://www.epa.gov (accessed on 13 September 2014).
20. Van Assen, V. Physics of City Buses and Their Environment. Master Thesis, University of Groningen, Groningen, The Netherlands, 2013.
21. *Inzetbaarheid Van Zero Emissie Bussen In Nederland*; Ministerie van Infrastructuur en Milieu, TNO, R10315; TNO: Den Hague, The Netherlands, 2015. (In Dutch)
22. Wolterink, S.; Bauer, P. High range on-line electric vehicles powered by Inductive Power Transfer. In Proceedings of the 2014 IEEE Transportation Electrification Conference and Expo (ITEC), Dearborn, MI, USA, 15–18 June 2014; pp. 1–7.
23. Jager, K.; Isabella, O.; Smets, A.H.M.; Van Swaaij, R.A.C.M.M.; Zeman, M. A Student Introduction to Solar Energy. Available online: https://courses.edx.org (accessed on 25 September 2014).
24. Sallan, J.; Villa, J.L.; Llombart, A.; Sanz, J.F. Optimal Design of ICPT Systems Applied to Electric Vehicle Battery Charge. *IEEE Trans. Ind. Electron.* **2009**, *56*, 2140–2149.
25. Chopra, S.; Bauer, P. Driving Range Extension of EV with On-Road Contactless Power Transfer—A Case Study. *IEEE Trans. Ind. Electron.* **2013**, *60*, 329–338.
26. De Doncker, R.W. Power electronic technologies for flexible DC distribution grids. In Proceedings of the 2014 International Power Electronics Conference (IPEC-Hiroshima 2014—ECCE-ASIA), Hiroshima, Japan, 18–21 May 2014; pp. 736–743.
27. Stamati, T.-E.; Bauer, P. On-road charging of electric vehicles. In Proceedings of the 2013 IEEE Transportation Electrification Conference and Expo (ITEC), Detroit, MI, USA, 16–19 June 2013; pp. 1–8.
28. Covic, G.A.; Boys, J.T. Modern Trends in Inductive Power Transfer for Transportation Applications. *IEEE J. Emerg. Sel. Top. Power Electron.* **2013**, *1*, 28–41.
29. Schlick, T.; Hagemann, B.; Kramer, M.; Garrelfs, J.; Rassmann, A. *Zukunftsfeld Energiespeicher*; Roland Berger: Munich, Germany, 2012. (In German)
30. Ko, Y.D.; Jang, Y.J. The Optimal System Design of the Online Electric Vehicle Utilizing Wireless Power Transmission Technology. *IEEE Trans. Intell. Transp. Syst.* **2013**, *14*, 1255–1265.
31. Pantic, Z.; Bai, S.; Lukic, S.M. Inductively coupled power transfer for continuously powered electric vehicles. In Proceedings of the Vehicle Power and Propulsion Conference, VPPC '09, Dearborn, MI, USA, 7–10 September 2009; pp. 1271–1278.
32. Verbeek, I.R.P.; Bolech, M.; Van Gijlswijk, R.N.; Spreen, I.J. TNO 2015 R10386. Energie en Milieu Aspecten Van Elektrische Personenvoertuigen. Available online: http://www.rvo.nl/actueel/nieuws/tno-elektrisch-rijden-tot-70-zuiniger (accessed on 15 October 2015). (In Dutch)

© 2016 by the authors; licensee MDPI, Basel, Switzerland. This article is an open access article distributed under the terms and conditions of the Creative Commons by Attribution (CC-BY) license (http://creativecommons.org/licenses/by/4.0/).